Refugia, colonization and diversification of an arid-adapted bird: coincident patterns between genetic data and ecological niche modelling

RAFAEL BARRIENTOS,*¶[1] LAURA KVIST,†¶ ANDRÉS BARBOSA,*[2] FRANCISCO VALERA,* FARES KHOURY,‡ SARA VARELA§ and EULALIA MORENO*

*Estación Experimental de Zonas Áridas (EEZA-CSIC), Ctra. de Sacramento s/n, La Cañada de San Urbano, E-04120 Almería, Spain, †Department of Biology, University of Oulu, POB 3000, FIN-90014 Oulu, Finland, ‡Department of Biology and Biotechnology, American University of Madaba, Madaba, Jordan, §Department of Ecology, Faculty of Science, Charles University, Viničná, 7, 128 44 Praha 2, Praha, Czech Republic

Abstract

Phylogeographical studies are common in boreal and temperate species from the Palaearctic, but scarce in arid-adapted species. We used nuclear and mitochondrial markers to investigate phylogeography and to estimate chronology of colonization events of the trumpeter finch *Bucanetes githagineus*, an arid-adapted bird. We used 271 samples from 16 populations, most of which were fresh samples but including some museum specimens. Microsatellite data showed no clear grouping according to the sampling locations. Microsatellite and mitochondrial data showed the clearest differentiation between Maghreb and Canary Islands and between Maghreb and Western Sahara. Mitochondrial data suggest differentiation between different Maghreb populations and among Maghreb and Near East populations, between Iberian Peninsula and Canary Islands, as well as between Western Sahara and Maghreb. Our coalescence analyses indicate that the trumpeter finch colonized North Africa during the humid Marine Isotope Stage 5 (MIS5) period of the Sahara region 125 000 years ago. We constructed an ecological niche model (ENM) to estimate the geographical distribution of climatically suitable habitats for the trumpeter finch. We tested whether changes in the species range in relation to glacial–interglacial cycles could be responsible for observed patterns of genetic diversity and structure. Modelling results matched with those from genetic data as the species' potential range increases in interglacial scenarios (in the present climatic scenario and during MIS5) and decreases in glacial climates (during the last glacial maximum, LGM, 21 000 years ago). Our results suggest that the trumpeter finch responded to Pleistocene climatic changes by expanding and contracting its range.

Keywords: *Bucanetes githagineus*, climate change, Mediterranean basin, microsatellites, mitochondrial DNA, range expansion

Received 7 October 2012; revision received 5 November 2013; accepted 6 November 2013

Correspondence: Rafael Barrientos, Fax: +34 925 265766;
E-mail: rafael.barrientos@uclm.es and Laura Kvist,
Fax: +35 885 531061; E-mail: laura.kvist@oulu.fi
[1]Present address: Área de Zoología, Departamento de Ciencias Ambientales, Facultad de Ciencias del Medio Ambiente, Universidad de Castilla-La Mancha, Avenida Carlos III, s/n, E-45071, Toledo, Spain
[2]Present address: Departamento de Ecología Evolutiva, Museo Nacional de Ciencias Naturales (MNCN-CSIC), José Gutiérrez Abascal, 2, E-28006, Madrid, Spain
¶The two-first authors have equally contributed to this article.

Introduction

The impact of Quaternary climatic oscillations on population processes of a plethora of boreal and temperate taxa has been studied in recent decades (reviewed in Taberlet *et al.* 1998; Hewitt 1999, 2004; Bennet & Provan 2008). In contrast, phylogeographical studies focused on arid-adapted animal species from southern regions (e.g. North Africa or Middle East) have remained scarce, with only a handful of published examples involving snails (Guiller

et al. 2001), mammals (e.g. Cosson *et al.* 2005; Nicolas *et al.* 2009; Ben Faleh *et al.* 2011), birds (e.g. Idaghdour *et al.* 2004; Guillaumet *et al.* 2006, 2008; García *et al.* 2008; Förschler *et al.* 2010) and, mainly, reptiles (e.g. Brown *et al.* 2002; Carranza *et al.* 2004, 2006; Rato *et al.* 2007, 2010), with none of them including niche modelling (see below). In this region, the role of successive expansions and contractions of the Sahara Desert in structuring populations (reviewed in Drake *et al.* 2011; see also Besnard *et al.* 2007; Guillaumet *et al.* 2006, 2008; Illera *et al.* 2008) is still debated and poorly understood. Even though the Sahara Desert may form an effective dispersal barrier at present, this has not always been the case. Biogeographical and paleohydrological studies show that the Sahara has been covered by dense river networks, for example, during Marine Isotope Stage 5 (hereafter, MIS5; 130 000–75 000 years ago) and at the beginning of the Holocene (11 000–8000 years ago), likely enabling several water-dependent species to cross the Sahara (Drake *et al.* 2011). Nevertheless, after the late Pleistocene, the Sahara became increasingly dry (Kröpelin *et al.* 2008). Moreover, the ongoing climate warming, combined with an increase in human pressure via, for example, agriculture and animal husbandry, can increase desertification (Le Houérou 2000). This may cause shifts in range not only in temperate species (Parmesan & Yohe 2003; Root *et al.* 2003), but also in species from semi-arid environments, which could be particularly at risk (Brown *et al.* 1997; Sanz 2002). Although these latter organisms are adapted to warm conditions, slight increases in aridity can cause their habitats to become unsuitable, for instance, due to the loss of the scarce water sources as a consequence of prolonged droughts, especially if this occurs during the breeding season (Allen & Saunders 2002).

The circum-Mediterranean region north of the Sahara is an acknowledged biodiversity hotspot (Myers *et al.* 2000), suggesting a complex evolutionary history for the region. Indeed, different colonization or radiation patterns have been described in North Africa: (i) westward expansion from Asia or the Middle East (Franck *et al.* 2001; Arnaiz-Villena *et al.* 2008; Illera *et al.* 2008), (ii) eastward from western or southwestern Maghreb (Carranza *et al.* 2004, 2006; Guillaumet *et al.* 2008) or even from the Canary Islands (Illera *et al.* 2011) and (iii) colonization from Europe (Guillaumet *et al.* 2006). These patterns suggest multiple refugia or origins, colonization routes and radiations for the species from the region.

The trumpeter finch (*Bucanetes githagineus*) is a small passerine (ca. 21 g) distributed throughout the semi-arid regions of the Western Palaearctic, from northwestern India throughout the Middle East to Western Sahara and the Canary Islands (Cramp & Perrins 1994), where it occupies semi-arid landscapes (Barrientos *et al.* 2009a). Based on plumage coloration and morphology, four

subspecies have been recognized (Cramp & Perrins 1994; see below). The species is expanding at the northwestern part of its range and has recently colonized Europe (Carrillo *et al.* 2007a; Barrientos *et al.* 2009b). Contrary to other species, whose expansions are assumed to have been human-mediated (e.g. Carranza *et al.* 2004; Cosson *et al.* 2005), the current range of the trumpeter finch seems to be a consequence of recent, natural expansion (Serra *et al.* 2006; Carrillo *et al.* 2007a). However, in some areas of the Near East, it is possible that the species is expanding in the most arid regions tracking human settlements that provide birds with water ad libitum (Cramp & Perrins 1994; Khoury & Al-Shamlih 2006).

The information available to explore past climatic conditions is continuously increasing (e.g. Waltari *et al.* 2007), and there is a recent tendency to integrate molecular ecology and modelling of past ranges to study the evolutionary histories of species (reviewed in Waltari *et al.* 2007; see also Hope *et al.* 2011; Rebelo *et al.* 2012). As no wide-scale land cover data with good resolution are yet available to reconstruct habitat traits in the past millennia, the best approach to date is to generate envelopes of climatic suitability, which assume that there is niche conservatism over time (Peterson *et al.* 1999).

In the present work, we used a phylogeographical approach complemented with ecological niche modelling (hereafter ENM) to trace the population history and colonization routes of the trumpeter finch and to match chronology of phylogeographical events within the species to global climatic changes (e.g. Hope *et al.* 2011; Rebelo *et al.* 2012). Specifically, we aimed to (i) determine the climatically suitable areas for the species during both glacial and interglacial periods, identifying where populations might have persisted in spite of Pleistocene climatic changes, and to track the colonization routes used by the species from ancient refuges; (ii) estimate dates of colonization and splitting events; and (iii) assess the population genetic structure of the current populations. For this purpose, we included 16 populations, totalling 271 birds (both fresh and museum specimens) across the species range. We used microsatellites and mitochondrial data to track recent range shifts and historical colonizations and diversification (Avise 2000). The ENM also allows us to identify which climatic variables were important in delimiting the range of our study species.

Material and methods

Study species

The trumpeter finch range is divided into three main regions with several smaller, patchy sites (Fig. 1). As most of their range has been poorly studied (Cramp & Perrins 1994; Del Hoyo *et al.* 2010), the knowledge on
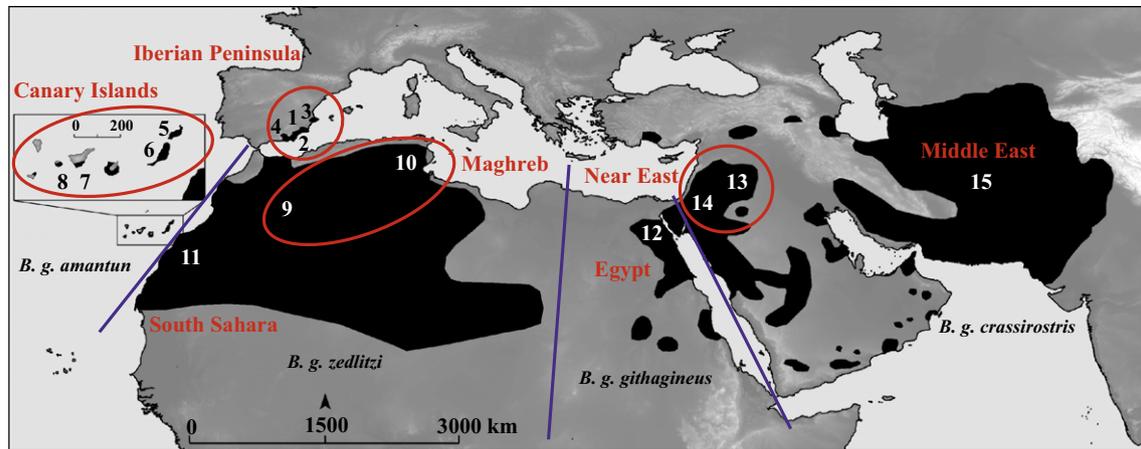
Fig. 1 Worldwide trumpeter finch range (based on Del Hoyo *et al.* 2010). The numbers represent the sampling localities. Gorafe = 1, Cabo de Gata = 2, Monnegre = 3, Tabernas = 4, Lanzarote = 5, Fuerteventura = 6, Tenerife = 7, La Gomera = 8, Morocco = 9, Tunisia & Algeria = 10, Western Sahara = 11, Egypt = 12, Jordan (two sites) = 13, Israel = 14, Iran = 15. The seven regions used to group the localities are also shown. The lines divide the subspecies described to date (Cramp & Perrins 1994).

connectivity among populations is still scarce (but see Barrientos *et al.* 2009b). Four subspecies are tentatively recognized based on plumage coloration and morphology (Cramp & Perrins 1994): *B. g. zedlitzi* in Mauritania, Maghreb, Libya and the Iberian Peninsula, perhaps also in northern Niger and northern Chad; *B. g. githagineus* in central and southern Nile Valley (Egypt), southeastern Egypt and northcentral and northeastern Sudan; *B. g. crassirostris* in Arabia, Sinai (Egypt), southcentral Turkey, Syria, Israel, Jordan, Iraq, Kuwait, Iran, Afghanistan, Uzbekistan, western Pakistan and northwestern India; and, *B. g. amantun* in the Canary Islands. The northern birds belonging to *B. g. zedlitzi* and *B. g. crassirostris* subspecies are larger than southern *B. g. githagineus* and *B. g. amantun* subspecies (Cramp & Perrins 1994). Colour variation in the northern subspecies is clinal, whereas it is more heterogeneous in the southern subspecies. The northern and southern subspecies are suggested to be mixed across their ranges in central Egypt (Cramp & Perrins 1994).

The species was first documented to breed in Europe in 1971 (García 1972). Its breeding range is expanding in southeastern Iberia (Carrillo *et al.* 2007a; Barrientos *et al.* 2009b), with several records outside of the breeding season in the western Mediterranean region (Spain, Llabrés 2010 or Italy, Gildi 1997), and even in North European countries such as Finland (Birdlife Finland 2008). This presence of individuals outside the current species range during the nonbreeding season precedes the establishment of new breeding sites in the periphery of its range (Barrientos *et al.* 2009b). Although the information is less detailed in Near East populations, it seems that the species began an expansion process there around 1950s (Cramp & Perrins 1994; Serra *et al.* 2006).

Sampling and laboratory protocols

We sampled 271 birds from 16 populations (Tunisia and Algeria were finally combined, see below; Fig. 1): four populations from the Iberian Peninsula (Gorafe, Cabo de Gata, Monnegre and Tabernas), four from Canary Islands (Lanzarote, Fuerteventura, Tenerife and La Gomera), three from Maghreb (Morocco, Algeria and Tunisia), one from south Sahara (Western Sahara), one from Egypt, two from the Near East (Jordan and Israel) and one from the Middle East (Iran). Samples include both fresh and museum samples. Fresh samples were obtained mainly by mist-netting, but also occasionally by sampling a single chick from every nest (see Barrientos *et al.* 2009b). Detailed information of sampling is given in Table S1 in Supporting Information and in Fig. 1.

DNA was extracted with the standard phenol–chloroform method (Sambrook & Russell 2001). Museum samples were extracted in a separate room using a fume hood with UV-light exposure prior to the extraction. Seven microsatellite loci – Lox1, Lox2 and Lox8 (Piertney *et al.* 1998), Ppi2 (Martínez *et al.* 1999), Pocc6 (Bensch *et al.* 1997), Pdo5 (Griffith *et al.* 1999) and Pk12 (GenBank Accession no. AF041466) – were amplified using the procedure detailed by Barrientos *et al.* (2009b). Microsatellites were run on ABI3730 and scored with GENEMAPPER v. 3.7 (Applied Biosystems, Foster City, CA, USA). Part of the mitochondrial control region was amplified using primers TrfinchL20 and passeriformesH830 (Kvist *et al.* 2011; Table S2, Supporting Information), which amplify most of domains I and II of the control region. The museum samples were amplified in two or three fragments using primers TrfinchL20 and TrfinchH465,

TrfinchL410 and PasseriformesH830, TrfinchL20 and TrfinchH262, TrfinchL208 and TrfinchH465, TrfinchL410 and TrfinchH649 or TrfinchL585 and PasseriformesH830 (Table S2, Supporting Information). PCR was performed in 10-μL volumes containing about 50 ng of template DNA (1–5 μL), 0.5 μM of each primer (0.5 μL each), 0.2 mM of each dNTP (1 μL), 1 μL of 10× PCR buffer (2.0 mM MgCl$_2$) and 0.06 μL of DNA-polymerase (Biotools, 5 U/μL). The PCR protocol was 94 °C for 2 min followed by 37 cycles of 94 °C for 30 s, 50 °C for 45 s and 72 °C for 30 s with a final extension in 72 °C for 5 min. The Egyptian samples required a secondary PCR using 1 μL of the primary PCR product as template. Sequencing of the PCR products was performed with BIGDYE v. 3.1 using primers TrfinchH262, TrfinchH465, TrfinchL410, TrfinchL585 or PasseriformesH830. Half of the museum samples were sequenced twice to check for consistency of the sequences. Sequencing reactions were run on an ABI3730. All sequences are available in GenBank (Accession nos. JX452830-JX453004 and JX453005-JX453016; see also Table S1, Supporting Information).

Microsatellite analyses

Locus Pk12 did not amplify in the Western Sahara samples, and therefore, this locus was removed from analyses where the Western Sahara was involved. We did not get good PCR products from some populations with museum samples, and therefore, these were excluded (see populations included in Table 1). We first used MICROCHEKER v. 2.2.3 (van Oosterhout *et al.* 2004) to check for null-alleles, large allele dropouts and scoring errors. The loci that showed evidence of null-alleles were removed from estimation of inbreeding coefficients, F_{IS}, calculated with Genepop (Raymond & Rousset 1995; Rousset 2008). The same program was used to calculate linkage disequilibrium for each pair of loci in each population. All loci were used to estimate basic diversity values, observed and expected heterozygosities (with ARLEQUIN v. 3.11; Excoffier *et al.* 2005) and allelic richness (with FSTAT v. 2.9.3; Goudet 2001) from each population sampled with at least 10 individuals.

In addition, we calculated the *M*-ratio (Garza & Williamson 2001) with Arlequin to detect possible bottlenecks or founder events. These demographic events can produce gaps in the size distribution of microsatellite alleles, which can be quantified as the *M*-ratio (or Garza–Williamson index), the mean ratio of the number of observed alleles to all the potential repeats within the allele size range across all loci. When seven or more loci are analysed, *M*-ratios below 0.68 suggest a reduction in population size (Garza & Williamson 2001; Excoffier *et al.* 2005). Population bottlenecks can cause genetic signatures in the distributions of allele sizes and generate an excess in expected heterozygosity as rare alleles that are lost from a population contribute little to

Table 1 Sample sizes for microsatellite data, observed (Ho) and expected (He) heterozygosities, allelic richness (*A*), Garza–Williamson index (*M*-ratio), results from testing for bottlenecks with the program Bottleneck (Wilcoxon test for heterozygote excess and mode shift test) and F_{IS} (over four loci) estimated from the microsatellite data. Values in regular text are estimated with six loci, and in italics with seven loci

Population (Region)	N	Ho (SD)	He (SD)	A	*M*-ratio (SD)	Wilcoxon test, Mode shift	F_{IS}
Gorafe (Iberian Peninsula)	26	0.5400 (0.2631)	0.7242 (0.3035)	2.88	0.708 (0.245)	NS, normal distribution	0.0541
		0.4939 (0.2694)	*0.6667 (0.3161)*		*0.750 (0.249)*	*NS, normal distribution*	NS
Tabernas (Iberian Peninsula)	51	0.5853 (0.2675)	0.7608 (0.2614)	3.01	0.804 (0.169)	NS, normal distribution	0.0627
		0.5442 (0.2673)	*0.7169 (0.2654)*		*0.832 (0.171)*	*NS, normal distribution*	NS
Cabo de Gata (Iberian Peninsula)	22	0.6057 (0.2839)	0.7534 (0.3027)	3.03	0.722 (0.238)	NS, normal distribution	−0.0139
		0.5668 (0.2789)	*0.7213 (0.2891)*		*0.762 (0.241)*	*NS, normal distribution*	NS
Monnegre (Iberian Peninsula)	16	0.5433 (0.3362)	0.7357 (0.3014)	2.96	0.616 (0.291)	NS, normal distribution	0.1097
		0.5514 (0.3077)	*0.7246 (0.2767)*		*0.647 (0.280)*	*NS, normal distribution*	NS
Lanzarote (Canary Islands)	25	0.6754 (0.2680)	0.7842 (0.2333)	3.07	0.654 (0.259)	*P* < 0.05, normal distribution	−0.0490
		0.6246 (0.2791)	*0.7253 (0.2638)*		*0.703 (0.269)*	*P < 0.01, normal distribution*	NS
Fuerteventura (Canary Islands)	26	0.6951 (0.2540)	0.7803 (0.2325)	3.05	0.680 (0.251)	*P* < 0.05, normal distribution	−0.0201
		0.6145 (0.3151)	*0.7148 (0.2740)*		*0.725 (0.258)*	*P < 0.05, normal distribution*	NS
Jordan (Near East)	28	0.5474 (0.2501)	0.7959 (0.2519)	3.12	0.756 (0.246)	*P* < 0.01, normal distribution	0.1098
		0.5218 (0.2381)	*0.7483 (0.2622)*		*0.790 (0.243)*	*P < 0.01, normal distribution*	NS
Morocco & Tunisia (Maghreb)	36	0.6731 (0.2596)	0.7749 (0.3045)	3.11	0.776 (0.167)	NS (*P* = 0.07), normal distribution	−0.0029
							NS
		0.6204 (0.2749)	*0.7333 (0.2990)*		*0.761 (0.166)*	*NS, normal distribution*	
Western Sahara (Western Sahara)	10	0.7913 (0.2509)	0.7912 (0.2148)	3.02	0.573 (0.344)	*P* < 0.01, shifted distribution	−0.2159
							NS

overall heterozygosity (Luikart & Cornuet 1998; Garza & Williamson 2001). We used BOTTLENECK v. 1.2.01 (Piry *et al.* 1999) to look for these signatures using the two-phase mutation model (with 70% of stepwise mutations) for microsatellites and examining the overall distribution of allele frequency classes ('mode shift' test) and using a Wilcoxon test to detect signs of excess of heterozygotes.

To measure genetic differentiation between populations, we calculated Jost's D_{est} (Jost 2008) with GENALEX 6.5 (Peakall & Smouse 2012). D_{est} is a relative measure of genetic differentiation, which has been shown to be less biased than F_{ST} for measuring differentiation, especially when the number of sampled individuals varies between populations (Gerlach *et al.* 2010). Significance for the D_{est}-values was obtained by 999 permutations. In addition, Arlequin (Excoffier *et al.* 2005) was used to estimate pairwise F_{ST}-values between the sampling sites for those sites from which at least seven individuals were sampled. The statistical significance was obtained by permuting the samples by 1000 permutations, and *P*-values were corrected with the Bonferroni step-down correction (Holm 1979). We chose only *F*-statistics and not *R*-statistics due to the relatively low sample size from some of the populations (Slatkin 1995; Gaggiotti *et al.* 1999). To test for isolation by distance (coordinates are shown in Table S3, Supporting Information), the pairwise distances between sampling sites, using Slatkin's linear F_{ST}, were correlated with logarithms of geographical distances using the matrix correlation test, the Mantel test, in Arlequin. Significance of correlation was tested with 1000 permutations. In addition, we used the molecular variance analysis (AMOVA) implemented in Arlequin to test for the best grouping of the populations. For this, we combined the samples from Iberia (Gorafe, Tabernas, Cabo de Gata and Monnegre) into one, as well as samples from Canary Islands (Fuerteventura and Lanzarote). We constructed nine different groups using three hierarchical levels, within populations, between populations and among groups. The nine groups were formed with the intention of testing all the possible connections between the populations taking into account the geographical locations of the populations. Significance was tested with 1000 permutations.

Population structure was further studied using STRUCTURE v. 2.2 (Pritchard *et al.* 2000; see also Falush *et al.* 2003). This program infers the number of populations (*K*) using a Markov chain Monte Carlo approach. We used no prior information of the sampling locations and assumed a model with population admixture and correlated allele frequencies within populations (Falush *et al.* 2003). We used 10 000 iterations as a burn-in and collected data for 100 000 iterations for a series of ten independent runs for each value of *K* between 1 and 10.

The likelihood of the data and subsequent log probabilities for the different numbers of subpopulations were calculated for each *K*. We also computed the posterior probabilities according to Bayes' Rule for each *K* (the Bayes factor) following the guidelines in the Structure manual. In addition, we applied the *ad hoc* method by Evanno *et al.* (2005), which is based on estimating ∆K between consecutive numbers of populations. The highest ∆K can be inferred as the best estimator of the actual *K*, and this method should detect the highest level of population structure even if several hierarchical levels exist (Evanno *et al.* 2005).

Mitochondrial analyses

The mitochondrial sequences were aligned by eye with Bioedit (Hall 1999). We constructed two data sets: one containing 576 bp long sequences from 175 individuals and one containing 194 bp from 187 individuals (due to the failure to sequence the whole fragment from twelve individuals, eight of them from Egypt). Diversity estimates including nucleotide diversity (π), theta (θ), number of haplotypes and haplotype diversity (ĥ) were calculated with DNASP v. 5.0 for both data sets (Librado & Rozas 2009). The following applies to the 576 bp data if not stated otherwise. We estimated the 'expansion parameters', Tajima's *D* and Fu's *F* and calculated raggedness index (*r*) and τ = 2 μ*t* (where μ is the mutation rate per generation and *t* time in generations) from mismatch distributions to detect possible changes in population size with DnaSP. The best substitution model for the data was estimated with Modelgenerator (Keane *et al.* 2006) according to Bayesian information criterion. This substitution model was used in analyses with Arlequin.

Pairwise Φ_{ST}-values between the study populations (sampled for more than seven individuals) were estimated with Arlequin using Tamura–Nei distance, and isolation by distance tested as described for microsatellites. AMOVA was performed as above, but using 16 different combinations instead of nine because the number of populations was larger in this data set. For this, we combined the samples from Iberia into one (Gorafe, Tabernas, Cabo de Gata and Monnegre), as well as samples from Near East (Jordan and Israel), Maghreb (Morocco, Tunisia and Algeria) and Canary Islands (Fuerteventura, Lanzarote, Tenerife and La Gomera). Egypt is represented by only two individuals.

To explore the colonization history in more detail, we used DIYABC v. 1.0.4.45 (Cornuet *et al.* 2008) to perform coalescence analyses. This program utilizes a coalescent-based approximate Bayesian computation algorithm to infer the population history by looking backwards in time to examine genealogy of alleles until the time at which the most recent common ancestor (hereafter

TMRCA) is reached. We carried out preliminary tests by building numerous different combinations of splitting and admixture along the scenarios starting from the six sampling regions (Fig. 1), that is, the Canary Islands, the Western Sahara, the Iberian Peninsula, Maghreb, the Near East (including Egypt, which did not deviate from the Near East population based on pairwise Φ_{ST}-values) and Iran at time 0 (present). We used prior historical information and geographical proximities of populations for building evolutionarily realistic scenarios. In addition, we performed a simplified run by combining the populations into three based on pairwise Φ_{ST}-values and geography: (i) Near East (including Egypt) and Middle East combined, (ii) Maghreb and Iberia combined and (iii) Western Sahara and Canary Islands combined. All three possible cladograms of a nonrooted tree were included in the scenarios. After the preliminary tests, we used altogether seven different historical scenarios for the final analysis (Fig. 2 shows the three best supported scenarios). We used a minimum substitution rate of 0.68×10^{-8} and maximum of 1.72×10^{-7} per generation based on conservative substitution rate estimates of 2–5% per Myr for the control region (Sato et al. 1999; Päckert et al. 2007) and a generation length (G) of 2.9 years for the trumpeter finch. Generation length was obtained from capture–recapture data in the Tabernas population (E. Moreno, unpublished data) and calculated using the equation $G = A + s/1\text{-}s$, where A is the age at first reproduction and s is the survival rate (Lande et al. 2003). Modelgenerator suggested that the Tamura–Nei substitution model was the best. However, the program crashed while trying to change the substitution model setting. Thus, we used Kimura two-parameter distance as an alternative. Priors used for effective population sizes were 100–1 000 000 and for splitting times from 1 to 5000 up to 5000 to 100 000, depending on the population. We simulated 7 000 000 data sets, which were compared to the observed data to choose the scenario that best explained the data by estimating posterior probabili-

ties for each scenario. We checked for the fit of observed and simulated summary statistics under the seven scenarios as recommended in the DIYABC manual for the following statistics: (i) for one sample statistics, we used the number of haplotypes and segregating sites, mean number of pairwise differences and its variance, Tajima's D, private segregating sites, mean numbers of the rarest nucleotide at segregating sites and its variance; and (ii) for two samples, we used the numbers of haplotypes and segregating sites, mean of pairwise differences and Φ_{ST}. In addition, we evaluated the confidence in scenario choice by estimating type I and II errors as suggested in the DIYABC manual. The scenario that best explained the data was used to estimate divergence times and effective population sizes. We used TCS v. 1.21 (Clement et al. 2000) for constructing the haplotype network.

Mitochondrial and microsatellite combined analyses

We also combined the microsatellite and mitochondrial data (576 bp fragment) for coalescence analysis with DIYABC (Cornuet et al. 2008). We used the same large-scale sample populations as above, except that we did not have microsatellite data from Iran and Egypt, so these sites were excluded (i.e. there were five populations: Iberia, Maghreb, Near East, Western Sahara and Canary Islands). We assumed a mutation rate of 1×10^{-5} for all the microsatellite loci (Kruglyak et al. 1998), otherwise the run conditions were as above. Prior distributions for effective population sizes and splitting times were as above, with slight modifications between the two runs performed. The simulated data were again compared to the observed data to choose the scenario that best explains the data. Posterior probabilities were estimated for each scenario, and the three best were chosen for a final run with 3 000 000 simulations (Fig. S1, Supporting Information). The scenario that best explained the data was used to estimate divergence times and effective population sizes.
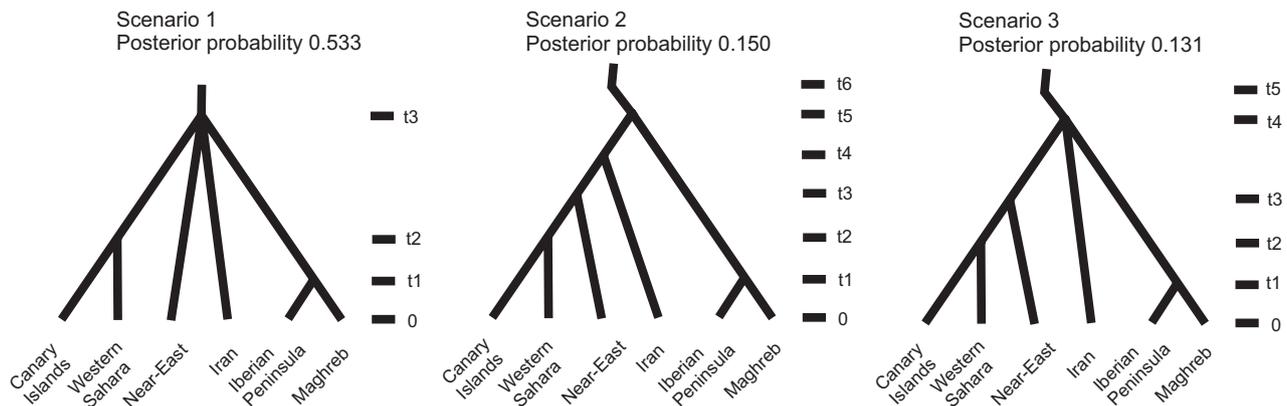
Fig. 2 Historical scenarios constructed for the coalescence analyses with mitochondrial (576 bp fragment) data.

Ecological niche modelling

We selected 197 species occurrences from the geo-referenced range map of the trumpeter finch from Fig. 1 (Table S4, Supporting Information; see also Fig. 5d). We used the 19 bioclimatic variables from WorldClim (version 1.4, see http://www.worldclim.org/ for variable descriptions). The WorldClim variables for the present interglacial scenario are the maps obtained by statistical interpolation of weather stations, with 30-arcsec (ca. 1-km) resolution (see Hijmans *et al.* 2005). For the Last Glacial Maximum (hereafter, LGM) cold scenario (21 000 years ago), we used the predictions of two general circulation models: the 'Community Climate System Model' (hereafter CCSM) and the 'Model for Interdisciplinary Research on Climate' (hereafter MIROC; version 3.2; downloaded from worldclim.org).

We modelled the current range of the trumpeter finch using the maximum entropy algorithm, MAXENT 3.3.3 (Phillips *et al.* 2006; Phillips & Dudik 2008), with the *R* library 'dismo' and the default settings (Hijmans *et al.* 2011). MAXENT calculates the climatic suitability of the species based on the species occurrence records and a set of background points, calibrating a model to discriminate between the species niche and the background conditions (used vs. available; Elith *et al.* 2006; Phillips *et al.* 2006). Model parameters were calibrated from 500 replicate model runs, where species records were randomly divided (80–20%) into 157 points for training the model and 40 points for testing the model predictions, plus 10 157 background points. Variable importance was determined from the percentage contribution of each variable to the model predictions. Overall model performance was evaluated using the area under the receiving operator characteristics curve (AUC), which ranges from 0.5 (randomness) to 1 (prefect prediction). The logistic output of MAXENT consists of a grid map with each cell having an index of suitability between 0 and 1. Low values indicate that conditions are climatically unsuitable for the species to occur, whereas high values indicate that conditions are suitable. We calibrated the model using the current range of the species, and we projected it into the two LGM cold climatic scenarios (21 000 years ago; that is, one of the most demanding scenarios for several species; see Introduction). We used a consensus approach to map the range of the species in the LGM. We projected the model in both general circulation models (CCSM and MIROC) and multiplied both maps. Thus, the LGM map shows the areas with high levels of climatic suitability for the species using both climatic models. We did not project the models to MIS5 (Last Interglacial Maximum, 126 000 years ago) because the currently available resolution of the climatic models for this period is still poor. Alternatively, we used the current climate conditions as a proxy of the MIS5 following Varela *et al.* (2009), because MIS5 matches the TMRCA (see below) and we wanted to explore climatic suitability for the trumpeter finch at that time.

Results

Microsatellite analyses

The highest expected heterozygosities were found in Jordan, Western Sahara, Fuerteventura and Lanzarote and the highest observed heterozygosities in Western Sahara, Lanzarote, Fuerteventura and Morocco. Allelic richness was the highest in Jordan and Morocco. All four populations from the Iberian Peninsula had diversity estimates somewhat lower than the other populations. Inbreeding coefficients estimated over four loci (Lox 2, Lox 8 and Pk12 were removed due to possible null-alleles) resulting in nonsignificant values for all populations (Table 1). No linkage disequilibrium was detected.

Bottleneck tests suggest a past bottleneck by revealing significant heterozygote excess in Lanzarote, Fuerteventura, Jordan and Western Sahara, which also showed a shifted allele size class distribution. *M*-ratio was low (below 0.68) in Monnegre, Lanzarote and Western Sahara (Table 1).

Pairwise D_{est}-values (Table 2), as well as F_{ST}-values (not shown), within the Iberian populations and within the Canary Islands were mostly nonsignificant (but Gorafe significantly differed from Tabernas) and close to zero. Significant differentiation based on D_{est}-values was observed between comparisons of most of the Iberian populations and the Canary Island populations. The Moroccan population differed significantly from two or three of the Iberian populations (depending on the number of loci used), from both Canary Island populations and from Western Sahara. Interestingly, differentiation was low across vast geographical distances, between Western Sahara and Jordan and between Morocco and Jordan. Isolation by distance was not detected ($r = 0.034$, $P > 0.5$). The hierarchical variance analysis resulted in the highest among-group variation when the Canary Island populations were considered as one group and all the others were combined. This grouping resulted in the highest and significant F_{CT}-value (Table S5, Supporting Information).

Structure gave the highest log probability for three clusters with a Bayes factor of 1.00 when data from six loci were used, but the application of the Evanno's method reduced the most likely number to two. When data from seven loci were used (excluding Western Sahara), the highest probability was obtained for six clusters (Bayes factor 1.00), whereas the Evanno's method still resulted in $K = 2$. Results from six loci are

Table 2 Pairwise D_{est}-values from six or seven (in italics) microsatellite loci above and Φ_{ST}-values from mitochondrial data (576 bp) below the diagonal for populations including at least 7 samples. Significant D_{est} and Φ_{ST}-values ($P < 0.05$) are shown in bold. Region abbreviations are as follows: Iber. Pen., Iberian Peninsula; Canar. Is., Canary Islands; West. Sah., Western Sahara

Population	Region	Gorafe	Tabernas	Cabo de Gata	Monnegre	Lanzarote	Fuerteventura	Jordan	Morocco	Tunisia & Algeria	Western Sahara
		Iber. Pen.	Iber. Pen.	Iber. Pen.	Iber. Pen.	Canar. Is.	Canar. Is.	Near East	Maghreb	Maghreb	West. Sah.
Gorafe	Iber. Pen.		**0.0334** *0.0275*	0.0049 *0.0142*	0.0581 *0.1026*	0.0958 *0.0627*	0.1006 *0.0638*	0.0929 *0.0693*	0.0599 *0.0429*	—	**0.2300**
Tabernas	Iber. Pen.	0.0051		0.0000 *0.0000*	0.0293 *0.0479*	0.0619 *0.0428*	0.0628 *0.0470*	0.0819 *0.0520*	0.0757 *0.0512*	—	**0.1684**
Cabo de Gata	Iber. Pen.	0.0031	−0.0238		0.0100 *0.0178*	0.0687 *0.0537*	0.0717 *0.0617*	0.0597 *0.0359*	0.0359 *0.0238*	—	**0.1761**
Monnegre	Iber. Pen.	0.0557	−0.0030	−0.0282		0.1215 *0.1402*	0.1138 *0.1468*	0.0740 *0.0765*	0.0802 *0.0891*	—	**0.1597**
Lanzarote	Canar. Is	**0.1545**	0.1059	0.0989	0.0140		0.0007 *0.0000*	0.1021 *0.0685*	0.0802 *0.0618*	—	**0.2362**
Fuerteventura	Canar. Is	**0.2735**	0.2060	0.2246	0.0985	−0.0138		0.0908 *0.0653*	0.1100 *0.0757*	—	**0.1978**
Jordan	Near East	**0.3414**	0.2704	0.2662	0.1442	0.0466	0.0423		0.0154 *0.0054*	—	0.0674
Morocco	Maghreb	0.0160	0.0583	0.0594	0.1315	0.2351	0.3383	0.4030		—	**0.1602**
Tunisia & Algeria	Maghreb	0.0170	−0.0285	−0.0044	−0.0145	0.0037	0.1020	0.1724	0.0707		—
Western Sahara	West. Sah.	**0.3397**	**0.2498**	**0.2965**	**0.1239**	−0.0008	−0.0218	−0.0027	**0.3998**	0.1866	—
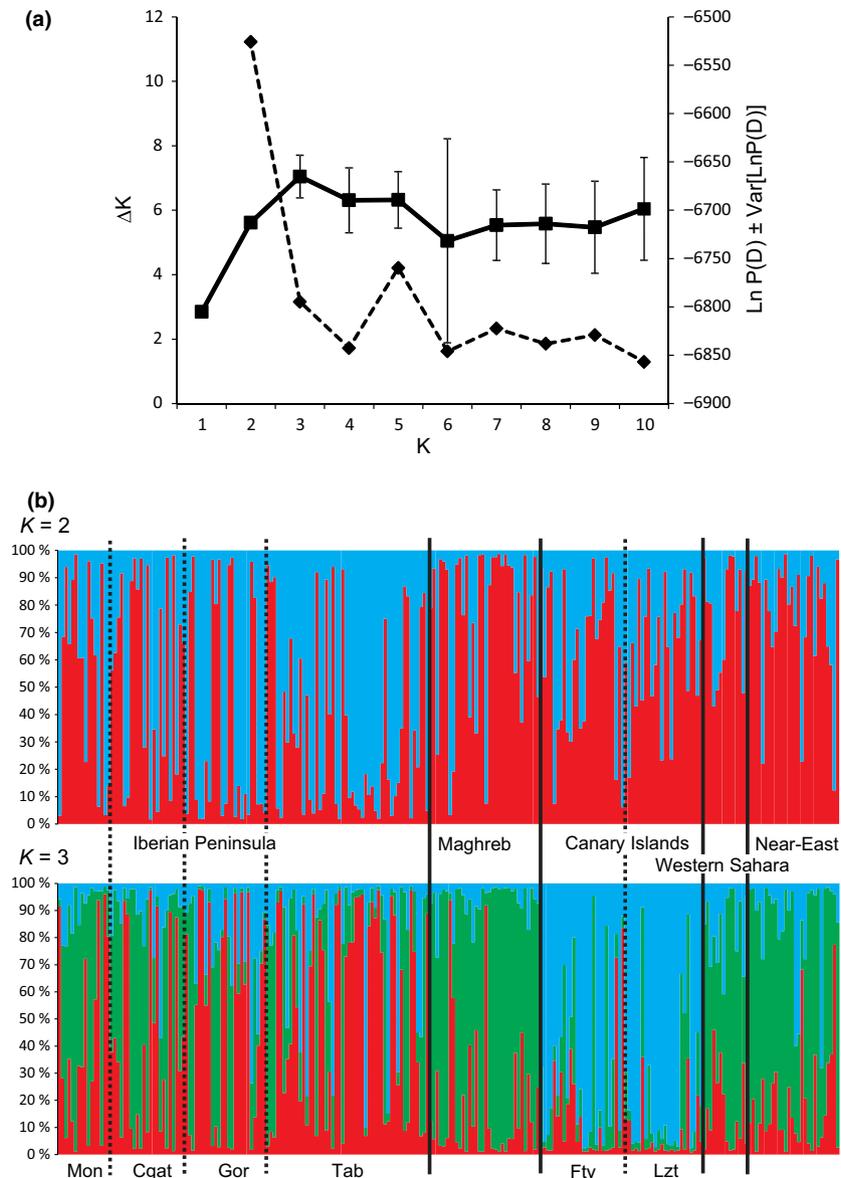
Fig. 3 Results from Structure analyses (a) ΔK- (dashed line) and likelihood values (solid line) for different numbers of populations (K) (b) bar plots of the Structure results with the highest K-values 2 and 3. Each individual is represented by a bar where the proportion of a membership in each population is shown by different colours. Individuals are grouped by their populations of origin, which are separated from each other by black, vertical lines over the two plots. Populations within Iberian Peninsula and Canary Islands are separated by dashed lines. Abbreviations are as follows: Monnegre = Mon, Cabo de Gata = Cgat, Gorafe = Gor, Tabernas = Tab, Fuerteventura = Ftv and Lanzarote = Lzt.

shown in Fig. 3. When the results suggested three separated clusters, most of the Iberian individuals as well as those from the Canary Islands fell into their own groups, but the third group included birds from Maghreb, Western Sahara and Near East. The number of populations inferred using the Evanno's approach for the six loci data set (two) showed no clear grouping according to the sampling locations. When the data set of seven loci was used, the samples from the Canary Islands grouped together, and others were mixed.

Mitochondrial analyses

We obtained 576 bp of the mitochondrial control region from 175 individuals. In addition, we sequenced 194 bp from twelve additional individuals (eight from Egypt, two from Tunisia, one from Algeria and one from Israel) from which we failed to sequence the whole 576-bp fragment. The sequences from the 175 individuals resulted in 76 different haplotypes with a mean nucleotide diversity of 0.00468. Haplotype network is shown in Fig. 4. The
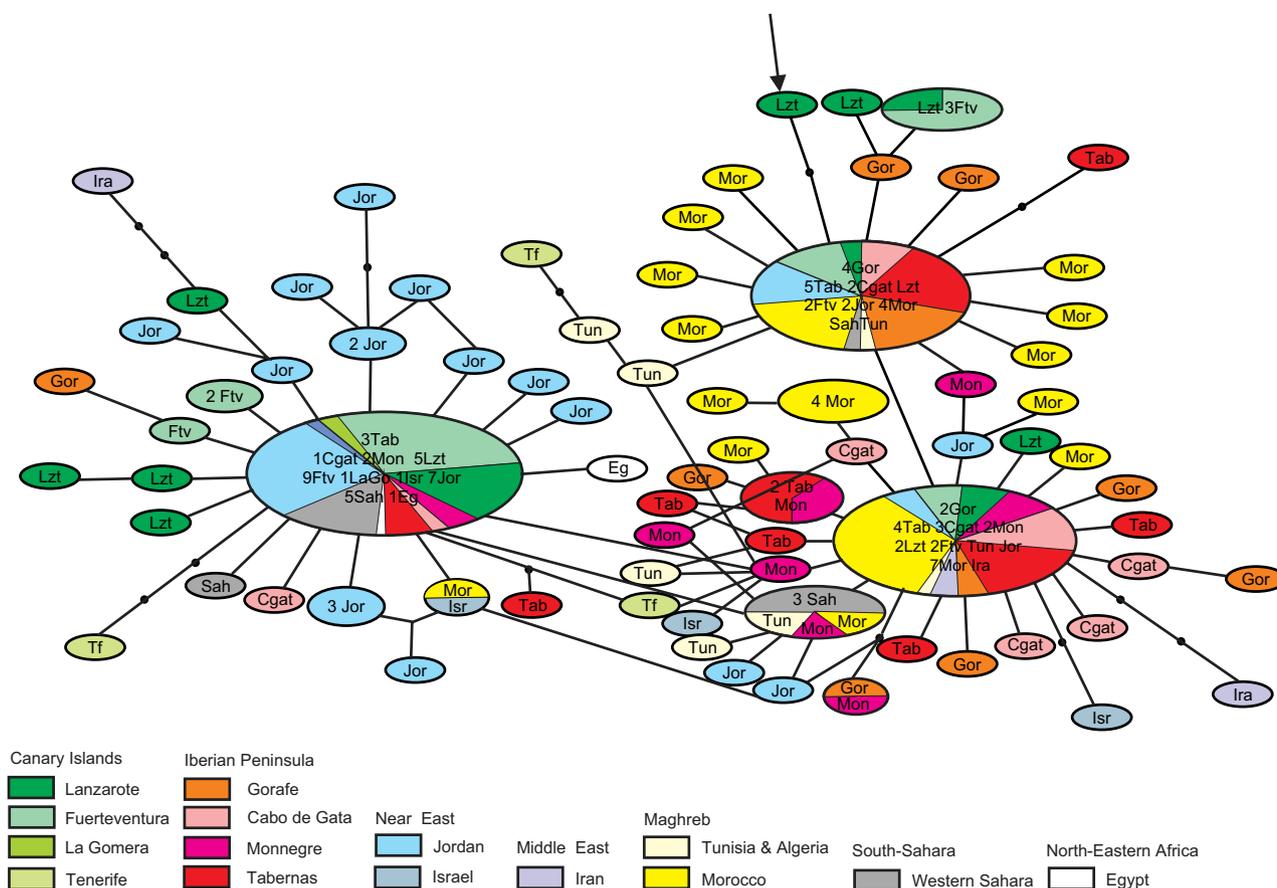
Fig. 4 Haplotype network of the mitochondrial control region sequences based on 576 bp from 175 individuals. Each population is marked with a different colour and abbreviations as shown in the figure. When there were more than one haplotype in the same population, their numbers are shown. Branching point of an outgroup *Carduelis hornemanni*, GenBank Accession no EU400528, is marked with an arrow.

highest nucleotide diversity was found in Iran (0.01042, $n = 3$) and the Near East (0.00436, $n = 31$; Jordan 0.00419, $n = 27$ and Israel 0.00550, $n = 4$), and the lowest from Egypt (0.00174, $n = 2$) and the Western Sahara (0.00197, $n = 10$; Table 3). The nucleotide diversities estimated from the 194-bp fragment from the populations with increased sample sizes were 0.00619 for Israel ($n = 5$) and 0.00309 for Egypt ($n = 10$); in Tunisia and Algeria, all haplotypes were identical ($n = 10$).

The parsimony network (Fig. 4) shows three main haplotypes found in most populations, but with different frequencies. These three haplotypes form centres of three connected starlike networks, indicating past population expansions. However, even though in many cases, θ-values of populations were much larger than nucleotide diversities (resulting in negative Tajima's D-values typical for expanded populations; Table 3), Tajima's D were significant only for the Iberian Gorafe and the Moroccan population. Fu's F-values, which are more sensitive to past expansions than Tajima's D, were significant for all Iberian and Maghreb populations,

Lanzarote and Jordan. Smooth, unimodal mismatch distributions from Tabernas, Gabo de Gata, Monnegre, Jordan, Morocco and Western Sahara indicated past population expansions, although the raggedness indexes were not significant.

Modelgenerator suggested the Tamura–Nei substitution model with invariable sites as the best model, with a fraction of invariable sites of 0.79. This model applied to pairwise Φ_{ST} calculations showed that Iberian subpopulations are not differentiated from each other, nor are the Canary Island and Near East subpopulations as all pairwise comparisons within these groups resulted in nonsignificant Φ_{ST}-values between populations. In the Maghreb group, Morocco was significantly different from pooled Tunisia and Algeria. Significant Φ_{ST}-values were also found between Iberian populations and most populations from Canary Islands, Jordan and Western Sahara. Two of the Iberian populations were significantly differentiated from Israel, Iran and Morocco. Notably, the Western Saharan population was significantly different from the Maghreb populations, but was not so from

Table 3 Sample sizes (*N*), genetic variation (ĥ = haplotype diversity, π = nucleotide diversity, θ = theta estimated from segregating sites) and parameters related to demography (Tajima's *D*, Fu's *F* and from mismatch distributions $\tau = 2\mu t$, where μ is mutation rate per generation and *t* time in generations and *r* = raggedness index) estimated from the mitochondrial DNA

Population	576 bp fragment					Demographic parameters			
	N	# hapl	ĥ	π	θ	Tajima's D	Fu's F	τ	r
Gorafe	14	10	0.923	0.00434	0.00711	−1.566 P < 0.05	−5.200 P < 0.01	2.010	0.0551 NS
Cabo de Gata	11	7	0.873	0.00297	0.00416	−1.156 NS	−4.704 P < 0.01	1.973	0.1117 NS
Monnegre	10	8	0.956	0.00382	0.00491	−0.958 NS	−4.698 P < 0.001	2.416	0.0889 NS
Tabernas	20	10	0.895	0.00377	0.00538	−1.060 NS	−4.191 P < 0.01	2.209	0.0507 NS
Iberian Peninsula	**55**	**26**	**0.906**	**0.00378**	**0.00912**	**−1.999 P < 0.05**	**−24.499 P < 0.001**	**2.174**	**0.0534 NS**
Lanzarote	16	11	0.908	0.00499	0.00628	−0.783 NS	−5.464 P < 0.01	3.213	0.0323 NS
Fuerteventura	19	6	0.754	0.00319	0.00298	0.225 NS	−0.598 NS	3.131	0.1059 NS
Tenerife	3	3	1.000	0.00926	0.00926	0.000 NS	0.458 NS	5.904	0.6667 NS
La Gomera	1	1	1.000	0.00000	0.00000	—	—	—	—
Canary Islands	**39**	**16**	**0.837**	**0.00430**	**0.00821**	**−1.583 NS**	**−7.977 P < 0.001**	**1.946**	**0.0518 NS**
Morocco	28	16	0.913	0.00346	0.00758	−1.885 P < 0.01	−12.627 P < 0.001	2.371	0.0771 NS
Tunisia &Algeria	7	7	1.000	0.00430	0.00425	0.056 NS	−5.015 P < 0.01	2.574	0.0907 NS
Maghreb	**35**	**20**	**0.924**	**0.00371**	**0.00843**	**−1.898 P < 0.05**	**−17.747 P < 0.001**	**2.134**	**0.0910 NS**
Egypt	**2**	**2**	**1.000**	**0.00174**	**0.00174**	**0.000 NS**	**0.000 NS**	**2.074**	**0.1364 P < 0.01**
Western Sahara	**10**	**4**	**0.711**	**0.00197**	**0.00245**	**−0.762 NS**	**−0.616 NS**	**1.133**	**0.1299 NS**
Jordan	27	17	0.926	0.00419	0.00676	−1.306 NS	−16.050 P < 0.001	2.559	0.0454 NS
Israel	4	4	1.000	0.00550	0.00568	−0.314 NS	−1.157 NS	3.742	0.1111 NS
Near East	**31**	**20**	**0.929**	**0.00436**	**0.00782**	**−1.632 NS**	**−18.966 P < 0.001**	**2.436**	**0.0388 NS**
Iran	**3**	**3**	**1.000**	**0.01042**	**0.01042**	**0.000 NS**	**0.588 NS**	**7.969**	**0.4444 NS**
Total	175	76	0.922	0.00468	0.01939	—	—	—	—

the Canary Island populations, and Egypt was not differentiated from Near East populations (Table 2). Contrary to microsatellite data, mitochondrial data show a significant isolation-by-distance pattern ($r = 0.239$, $P < 0.05$).

The hierarchical molecular analyses with fifteen different groupings partitioned the largest amount of variance between groups when Iberia was combined with Maghreb, Canary Islands with Western Sahara, Near East with Egypt and Iran treated separately (21.3%). This grouping also resulted in the highest F_{CT}-value and a low F_{SC}-value (Table S6, Supporting Information).

Coalescence analyses

When only the 576 bp mitochondrial data were used in DIYABC analyses, the best of seven historical scenarios was scenario 1 in Fig. 2. This scenario included the first split between Iberia and Maghreb at t1, the second split between Western Sahara and Canary Islands at t2 and the third at t3 including a simultaneous split of four branches leading to Iran, to the Near East, to the Western Sahara-Canary Islands and to Maghreb-Iberia. Posterior probability using logistic regression resulted in 0.53 for this scenario, and the second best (scenario 2 in Fig. 2) had a posterior probability of 0.15. Comparison of summary statistics of the observed data with the summary statistics obtained according to each of the seven simulated scenarios did not lend clear support to

any of the scenarios; most of the statistics were within the ranges of the simulated ones. Type I error (the true scenario did not have the highest probability) was 0.148, and the mean of type II errors (the false scenario is not rejected) was 0.070. The best scenario for the combined microsatellite and mitochondrial data was quite similar to that obtained only with mitochondrial data (scenario 1 in Fig. S1, Supporting Information; logistic regression 0.43; t3, i.e. TMRCA, was 125 000 years ago with combined data), but the estimated error rates remained high with 0.312 for type I and 0.295 for type II errors. Posterior estimates for splitting times and effective population sizes from mitochondrial analyses are shown in Table 4.

Ecological niche modelling and climate change

Our model showed a high power of discrimination between presences and background, with an AUC for the calibrating data set of 0.87 (i.e. 87% of the records were correctly predicted). Thus, our model was highly accurate and its prediction was significantly greater than the random one (AUC = 0.5, one-tailed Wilcoxon signed rank test; $P = 0.002$). Moreover, our model correctly predicted the validation data set, AUC = 0.80, which indicates that our model did not overfit.

Our analysis indicated that climatic suitability is directly proportional to the temperature in summer

Table 4 Posterior estimates of splitting times and effective population sizes (modes) with 95% highest posterior densities in parentheses from mitochondrial coalescence analyses with DIYABC. Estimates are for scenario 1 in Fig. 2. Time estimates are in years

Parameter	Estimate
N_e Iberia	9.73×10^5 (1.95×10^5–9.87×10^5)
N_e Maghreb	3.83×10^5 (1.09×10^5–9.79×10^5)
N_e Canary Islands	3.44×10^5 (1.28×10^5–9.87×10^5)
N_e Western Sahara	1.46×10^5 (6.07×10^4–9.56×10^5)
N_e Near East	6.54×10^5 (2.65×10^5–9.71×10^5)
N_e Iran	4.23×10^5 (7.94×10^4–9.76×10^5)
t1 (split Iberia/Maghreb)	4.83×10^3 (1.48×10^3–4.98×10^3)
t2 (split C-Islands/ W-Sahara)	5.53×10^3 (1.43×10^3–1.83×10^4)
t3 (TMRCA of the study populations: split Iberia+Maghreb/Iran/ N-East/C- Islands+W-Sahara)	8.67×10^3 (2.81×10^3–4.14×10^4)

(BIO9; importance of 28%), the precipitation seasonality (BIO15; 15%) and the winter mean temperature (BIO11; 13%), with the climatic suitability being highest at around 18 °C in this last variable. Thus, our model showed that the species climatic requirements are related to warm and dry conditions.

The present potential range based on climatic variables (Fig. 5a) is basically consistent with the observed current range (Fig. 1). The map showed that the most suitable conditions are concentrated in the Middle East and the northwestern Africa. It is outstanding that the large gap present in the trumpeter finch range in inland Egypt and Libya (Fig. 1) was also detected with ENM (Fig. 5a), suggesting that there are no suitable climatic conditions for the species to survive in those areas. Climatic suitability is intermediate to high in some areas where the species has not been recorded like Turkey, coastal Egypt and Libya, East Iran or the central Iberian Peninsula.

The estimated climatic suitability for the trumpeter finch during the LGM underwent a general range contraction, with the main area of suitable habitat identified in Iran, Iraq, Syria, Jordan, Saudi Arabia, southeastern Morocco, Algeria and Niger (Fig. 5b). These refugia were likely isolated, with at least the Maghreb population isolated from the easternmost nuclei. Comparing the model predictions between glacial and interglacial scenarios, we observed that, globally, the climatic suitability for the species had increased (Fig. 5c). Both area expansion and an increase in local climatic suitability have occurred after the glacial maximum, suggesting that the species could have experienced an expansion associated with this climatic warming. Finally, we created a map to identify the areas that showed climatically suitable conditions for the species in both glacial and interglacial scenarios (Fig. 5d). We consider that those areas could have been the climatic refugia for the species during the
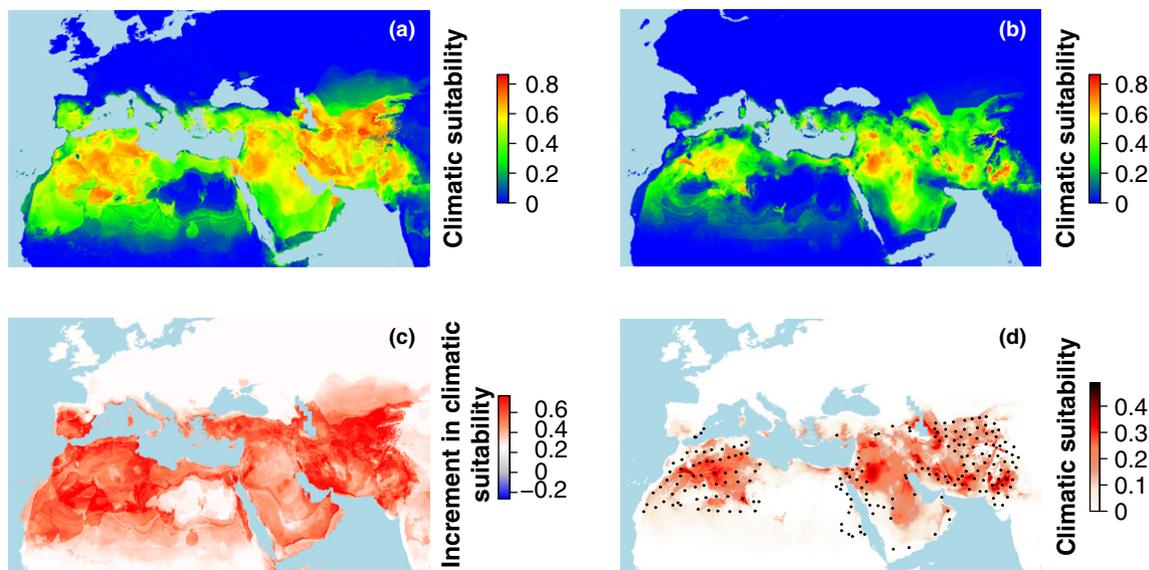
Fig. 5 Species climatic suitability in the present interglacial scenario (a), and during the LGM (b). Increment in climatic suitability from glacial to interglacial periods (c), obtained from subtracting habitat suitability in LGM (a) from the present scenario (b). Climatic suitability during glacial–interglacial cycles (d). Red areas indicate the locations that showed suitable conditions for the species during both glacial and interglacial scenarios. Black dots show the current species occurrences used in our analyses (see Table S4 in Supporting Information).

Pleistocene as climatic conditions were more stable there. These areas are located in Iran, Jordan, north Arabia and southwestern Maghreb (Morocco). The high number of localities where the species is currently present, but that are placed outside of these potential refugia (black dots from Fig. 5d and Table S4, Supporting Information), highlights that the species has expanded its geographical range since the LGM.

Discussion

Trumpeter finch diversification

With mitochondrial data, we detected signs of past population expansions in populations from the Iberian Peninsula, the Near East, Morocco, and combined Tunisia and Algeria. These signs of expansion are likely of an older origin than the recent expansions recorded in the Near East and Iberia (López-Seoane 1861; Vayreda 1883; García 1972; Khoury & Al-Shamlih 2006). Values of τ from the mismatch distributions (Table 3) indicate that these expansions had already occurred 220 000–68 000 years ago (estimated using divergence rates of 2–5%/Myr and τ-values from 1.97 to 2.55; from lower range in Gabo de Gata, southeastern Iberian Peninsula, to upper range in Jordan, respectively), likely reflecting an expansion in the ancestral population. This period overlaps with the humid period during MIS5 (130 000–75 000 years ago) in the Sahara region. The TMRCA of trumpeter finch populations was estimated at about 125 000 years ago with the combined mitochondrial and microsatellite data set. These estimates indicate that the common ancestor existed shortly before the humidification of the Sahara, which facilitated the expansion and spread of the species across North Africa (see Drake *et al.* 2011 for other examples from this humid phase). High diversity and large τ-values in populations from the Near and the Middle East indicate that the colonization occurred from east to west, but topologies of the phylogenetic trees (best coalescent scenarios, Fig. 2) or the maximum parsimony network (Fig. 4) do not lend support to any direction. Westward colonization would agree with results from Arnaiz-Villena *et al.* (2008), who suggest that Asia is the most likely origin for the 'Arid-Zone' Carduelini finches, a group including the trumpeter finch. According to these authors, the split between the trumpeter finch and its closely related sister-species, the Mongolian finch (*B. mongolica*), occurred about 6.5 Mya.

The present North African populations are differentiated in mitochondrial markers (pairwise Φ_{ST}-values 0.3998 between Western Sahara and Morocco and 0.1866 between Western Sahara and Tunisia and Algeria combined) and in microsatellite loci (pairwise D_{est}

between Western Sahara and Morocco 0.1602, but pairwise F_{ST}-value between Western Sahara and Morocco was nonsignificant). This differentiation could have resulted from at least two scenarios. First, the species could once have been distributed across a wider range in northwestern Africa, when the region was moister. For instance, Guillaumet *et al.* (2006, 2008) found that steep increases in aridity in Africa are coincident with north–south vicariance events mediated by the Sahara in the *Galerida* larks, a group of arid-adapted birds. Similarly, populations of smooth snakes *Macroprotodon* sp. in southern Morocco and coastal Western Sahara, where habitats are more suitable than further inland, have been suggested to be relicts from more mesic periods (Carranza *et al.* 2004). Saharan cycles of desert expansion and retraction may have also provided the conditions for population bottlenecks leading to radiation in West African *Taterillus*, rodents living in subdesert habitats (Dobigny *et al.* 2005). When the Sahara expanded after aridity increased, populations of the trumpeter finch became isolated. However, there are still remnants of shared ancestral polymorphism in these populations. For instance, we found a statistically significant divergence based on mitochondrial analyses between the geographically nearby populations of Morocco and Tunisia and Algeria combined, even though they share common haplotypes, supporting a common history followed by segregation. It is worth mentioning that this pattern of genetic differentiation between Morocco and Tunisia based on mitochondrial data has also been found in Dupont's lark *Chersophilus duponti* (García *et al.* 2008), a passerine living in subdesert steppes, as well as in several other arid-adapted species (reviewed in Barata *et al.* 2008), suggesting a common process at a regional scale. A second possibility is that the species colonized northwestern Africa using two routes: one north of the Sahara and another south of the Sahara, which can also explain the observed differentiation in North Africa. The two colonization routes might meet somewhere between our sampling sites from the Western Sahara and Morocco. Mitochondrial differentiation is stronger between Morocco and the Western Sahara than between Morocco and samples from Tunisia and Algeria, suggesting a closer connection between the northernmost African populations. In addition, populations as distant as the Near East and the Western Sahara are not differentiated from each other, which may result from the Near East having served as a source for colonization in the Western Sahara (or vice versa), supporting this second explanation of colonization around the Sahara. A secondary contact of the two colonization routes would likely also result in elevated diversity values in populations located in the zone, which we did not detect. This does not completely rule

out the possibility of existence of a contact zone, because it is possible that our sampling sites are not located directly in the zone, as there is actually a 1000-km gap between the sampling sites in the Western Sahara and Morocco. In any case, the genetic structure we found does not support the four trumpeter finch subspecies recognized to date based on plumage coloration and morphology (Cramp & Perrins 1994).

Pairwise F_{ST}- and Φ_{ST}-values (negative values for both) and AMOVA analyses support close connectivity of the Western Sahara and Canary Islands and differentiation between Morocco and the Canary Islands. On the other hand, D_{est}-values were higher between the Western Sahara and the Canary Islands than between Morocco and the Canary Islands. These islands, a volcanic archipelago that has never been connected to the continent (Illera *et al.* 2012), were likely colonized from a source located in the present northwestern Africa (although it is possible that colonization has also occurred the other way round, from the Canary Islands to continental Africa; see Illera *et al.* 2011). Our results give more support to colonization from a region around the Western Sahara than from Morocco (F_{ST}- and Φ_{ST}-values, AMOVA and coalescence analyses), but not decisively (D_{est}-values). Coalescence time suggests that divergence of Canary Island from Western Sahara populations occurred about 5500 years ago. The increased aridification of the westernmost part of the Sahara region in the late Pleistocene–early Holocene could have been one of the driving forces for the colonization of the Canary Islands. At that time, the current Sahara Desert was either steppe at low elevation, or temperate xerophytic woods/scrub (Jolly *et al.* 1998), but since 5500 years ago aridification increased, resulting the desert we know today around 2700 years ago (Kröpelin *et al.* 2008). Aridification in semi-arid landscapes not only reduced water availability but also changed vegetation composition, likely affecting the trumpeter finch as well, even though it has been described as a 'facultative drinker' (as defined by Bartholomew 1972; MacMillen 1990) because it maximizes water intake when foraging on seeds (Carrillo *et al.* 2007b). Naturally, it is also possible that the Canary Islands were colonized by chance via jump dispersal without any habitat-related effects.

We found evidence of recent bottlenecks in Lanzarote and Fuerteventura. The heterozygote excess method implemented in Bottleneck should be able to detect a bottleneck of $N_e = 50$ for 25–250 generations (0.25–2.5 times $2N_e$; Cornuet & Luikart 1996) and M-ratios for a few hundred generations (Garza & Williamson 2001) after the initiation of the bottleneck. The bottlenecks detected from the Canary Islands cannot therefore reflect a founder event, but instead some other event that has reduced population sizes during historical times. The detection of a bottleneck also in the geographically nearby Western Sahara population may imply some common event for the region, although sample size is low and could constrain our findings.

The split between Maghreb and Iberia was dated as the most recent splitting event, about 4800 years ago. This timing seems quite old, as the trumpeter finch was first detected in southwestern Europe in the middle of the 19th century (López-Seoane 1861; Vayreda 1883), and first breedings were recorded as late as in the second half of the 20th century (García 1972). However, it is also possible that the population in Iberia could have persisted for a longer time remaining undetected or, more likely, that differentiation could already have occurred in the North African continent. In addition, incomplete lineage sorting, which can be seen throughout the studied range, confuses the timing of population splits. The case of the trumpeter finch mirrors that of the Dupont's lark, which remained unnoticed in Europe until the 19th century (Viellot 1820), but whose Iberian and Moroccan populations diverged, based on genetic data, 24 000 years ago (García *et al.* 2008). Whether the recent range expansions are a consequence of climate change (Carrillo *et al.* 2007a), human-induced habitat changes (Khoury & Al-Shamlih 2006) in the source or receiving area, or have happened just by chance, remains unknown. However, it is likely that the colonization has occurred by many individuals or it is still on-going as no bottlenecks, indicating the reduction in population sizes through recent founder events were detected (see also Barrientos *et al.* 2009b).

Ecological niche modelling and its congruence with genetic data

According to our models, the species should have had a wide range during the warm scenarios and should decrease their potential area in the glacial cycles. During MIS5, the climatic conditions were similar to the present (Varela *et al.* 2009), which support the expansion of the most recent common ancestor across a range similar to the current one (see also Drake *et al.* 2011). Subsequently, the climate became colder during the glaciations, and the trumpeter finch became isolated in several refugia like Iran, Iraq, Syria, Jordan, Saudi Arabia, southeastern Morocco, Algeria and Niger during LGM. This fact can lead to differences in genetic structure between geographically close populations. For instance, eastern Maghreb (Tunisia), a region that did not retain suitable climatic conditions during LGM, is genetically different from southwestern Maghreb (Morocco) as has also been seen in some other arid-adapted species (see above). The lack of differentiation between most of the continental populations based on

microsatellites could be explained by a recovery of climatic suitability in more recent times, and the subsequent population expansion across Asia, Africa and Europe. The climatic suitability found with ENM for the present is intermediate to high in some areas where the species has not been recorded (e.g. most of Turkey, coastal Egypt and Libya or northwestern Iran). The absence of occurrence data in a priori climatically suitable areas is likely due to the fact that the species has been poorly searched in several regions or, alternatively, could be related to dispersal limitations or biotic interactions. Future field work should add information to this open question and give more clues about the variables (other than climate-related ones) that are affecting the observed geographical expansion. Climatic suitability is also high in the central Iberian Peninsula, where it is known that the species is currently absent (Manrique *et al.* 2003), but which can be considered a potential region for continuing the on-going expansion of the trumpeter finch (Carrillo *et al.* 2007a).

On the basis of our genetic data complemented with ENM, we can conclude that both recent expansion in border regions and ancient colonization of North Africa, including later colonization of the Canary Islands, seem to have followed, at least partially, climatic events.

References

Allen CR, Saunders DA (2002) Variability between scales: predictors of nomadism in birds of an Australian Mediterranean climate system. *Ecosystems*, **5**, 348–359.

Arnaiz-Villena A, Moscoso J, Ruiz-del-Valle J *et al.* (2008) Mitochondrial DNA phylogenetic definition of a group of 'arid-zone' Carduelini finches. *The Open Ornithology Journal*, **1**, 1–7.

Avise JC (2000) *Phylogeography: The History and Formation of Species*. Harvard University Press, Cambridge, Massachusetts, USA.

Barata M, Harris DJ, Castilho R (2008) Comparative phylogeography of northwest African *Natrix maura* (Serpentes: Colubridae) inferred from mtDNA sequences. *African Zoology*, **43**, 1–7.

Barrientos R, Valera F, Barbosa A, Carrillo CM, Moreno E (2009a) Plasticity of nest-site selection in the trumpeter finch: a comparison between two different habitats. *Acta Oecologica*, **35**, 499–506.

Barrientos R, Kvist L, Barbosa A, Valera F, López-Iborra GM, Moreno E (2009b) Colonization patterns and genetic structure of peripheral populations of the trumpeter finch (*Bucanetes githagineus*) from Northwest Africa, the Canary Islands and the Iberian Peninsula. *Journal of Biogeography*, **36**, 210–219.

Bartholomew GA (1972) The economy of seed-eating birds that survive without drinking. In: *Proceedings of the 15th International Ornithological Congress* (ed. Voous KH), pp. 237–254. EJ Brill, Leiden, Netherlands.

Ben Faleh AR, Granjon L, Tatard C, Ben Othmen A, Said K, Cosson JF (2011) Phylogeography of the Greater Egyptian Jerboa (*Jaculus orientalis*) (Rodentia: Dipodidae) in Mediterranean North Africa. *Journal of Zoology*, **286**, 208–220.

Bennet KD, Provan J (2008) What do we mean by 'refugia'? *Quaternary Science Reviews*, **27**, 2449–2455.

Bensch S, Price T, Khon J (1997) Isolation and characterization of microsatellite loci in a *Phylloscopus* warbler. *Molecular Ecology*, **6**, 91–92.

Besnard G, Rubio de Casas R, Vargas P (2007) Plastid and nuclear DNA polymorphism reveals historical processes of isolation and reticulation in the olive tree complex (*Olea europaea*). *Journal of Biogeography*, **34**, 736–752.

Birdlife Finland (2008) Available from: http://www.birdlife.fi/havainnot/lintutilanne/hav-2008-06-17.shtml.

Brown JH, Valone TJ, Curtin CG (1997) Reorganization of an arid ecosystem in response to recent climate change. *Proceedings of the National Academy of Science of USA*, **94**, 9729–9733.

Brown RP, Suárez NM, Pestano J (2002) The Atlas mountains as a biogeographical divide in North–West Africa: evidence from mtDNA evolution in the Agamid lizard *Agama impalearis*. *Molecular Phylogenetics and Evolution*, **24**, 324–332.

Carranza S, Arnold EN, Wadec E, Fahd S (2004) Phylogeography of the false smooth snakes, *Macroprotodon* (Serpentes, Colubridae): mitochondrial DNA sequences show European populations arrived recently from Northwest Africa. *Molecular Phylogenetics and Evolution*, **33**, 523–532.

Carranza S, Arnold EN, Pleguezuelos JM (2006) Phylogeny, biogeography and evolution of two Mediterranean snakes, *Malpolon monspessulanus* and *Hemorrhois hippocrepis* (Squamata, Colubridae) using mtDNA sequences. *Molecular Phylogenetics and Evolution*, **40**, 532–546.

Carrillo C, Barbosa A, Valera F, Barrientos R, Moreno E (2007a) Northward expansion of a desert bird: effects of climate change? *Ibis*, **149**, 166–169.

Carrillo CM, Moreno E, Valera F, Barbosa A (2007b) Seed selection by the trumpeter finch, *Bucanetes githagineus*. What currency does this arid-land species value? *Annales Zoologici Fennici*, **44**, 377–386.

Clement M, Posada D, Crandall KA (2000) TCS: a computer program to estimate gene genealogies. *Molecular Ecology*, **9**, 1657–1660.

Cornuet JM, Luikart G (1996) Description and power analysis of two tests for detecting recent population bottlenecks from allele frequency data. *Genetics*, **144**, 2001–2014.

Cornuet JM, Santos F, Beaumont MA *et al.* (2008) Inferring population history with DIY ABC: a user-friendly approach to Approximate Bayesian Computations. *Bioinformatics*, **24**, 2713–2719.

Cosson JF, Hutterer R, Libois R, Sarà M, Taberlet P, Vogel P (2005) Phylogeographical footprints of the Strait of Gibraltar and Quaternary climatic fluctuations in the western Mediterranean: a case study with the greater white-toothed shrew, *Crocidura russula* (Mammalia: Soricidae). *Molecular Ecology*, **14**, 1151–1162.

Cramp S, Perrins CM (1994) *Handbook of the Birds of Europe the Middle East and North Africa. The Birds of the Western Palearctic*, Vol. VII. Oxford University Press, New York, USA.

Del Hoyo J, Elliott A, Christie DA (2010) *Handbook of the Birds of the World. Weavers to New World Warbles*, Vol. 15. Lynx Editions, Barcelona, Spain.

Dobigny G, Aniskin V, Granjon L, Cornette R, Volobouev V (2005) Recent radiation in West African *Taterillus* (Rodentia, Gerbillinae): the concerted role of chromosome and climatic changes. *Heredity*, **95**, 358–368.

Drake NA, Blench RM, Armitage SJ, Bristow CS, White KH (2011) Ancient watercourses and biogeography of the Sahara explain the peopling of the desert. *Proceedings of the National Academy of Science of USA*, **108**, 458–462.

Elith J, Graham CH, Anderson RP *et al.* (2006) Novel methods improve prediction of species' distributions from occurrence data. *Ecography*, **29**, 129–151.

Evanno G, Regnaut S, Goudet J (2005) Detecting the number of clusters of individuals using the software STRUCTURE: a simulation study. *Molecular Ecology*, **14**, 2611–2620.

Excoffier L, Laval G, Schneider S (2005) Arlequin ver. 3.0: an integrated software package for population genetics data analysis. *Evolutionary Bioinformatics Online*, **1**, 47–50.

Falush D, Stephens M, Pritchard JK (2003) Inference of population structure using multilocus genotype data: linked loci and correlated allele frequencies. *Genetics*, **164**, 1567–1587.

Förschler MI, Khoury F, Bairlein F, Aliabadian M (2010) Phylogeny of the mourning wheatear *Oenanthe lugens* complex. *Molecular Phylogenetics and Evolution*, **56**, 758–767.

Franck P, Garnery L, Loiseau A *et al.* (2001) Genetic diversity of the honeybee in Africa: microsatellite and mitochondrial data. *Heredity*, **86**, 420–430.

Gaggiotti OE, Lange O, Rassmann K, Gliddon C (1999) A comparison of two indirect methods for estimating average levels of gene flow using microsatellite data. *Molecular Ecology*, **8**, 1513–1520.

García L (1972) Primera nidificación verificada de *Rhodopechys githaginea* en el suroeste de Europa. *Ardeola*, **16**, 215–222.

García JT, Suárez F, Garza V, Calero-Riestra M, Hernández J, Pérez-Tris J (2008) Genetic and phenotypic variation among geographically isolated populations of the globally threatened Dupont's lark *Chersophilus dupontii*. *Molecular Phylogenetics and Evolution*, **46**, 237–251.

Garza JC, Williamson EG (2001) Detection of reduction in population size using data from microsatellite loci. *Molecular Ecology*, **10**, 305–318.

Gerlach G, Jueterbock A, Kraemer P, Deppermann J, Harmand P (2010) Calculations of population differentiation based on GST and D: forget GST but not all of statistics!. *Molecular Ecology*, **19**, 3845–3852.

Gildi R (1997) Osservazione di un Trombettiere *Bucanetes githagineus* nel Lazio. *Alula*, **4**, 101.

Goudet J (2001) FSTAT, a program to estimate and test gene diversities and fixation indices (version 2.9.3). Available from: http://www.unil.ch/izea/softwares/fstat.html

Griffith SC, Stewart IRK, Dawson DA, Owens IPF, Burke T (1999) Contrasting levels of extra-pair paternity in mainland and island populations of the house sparrow (*Passer domesticus*): is there an island effect? *Biological Journal of the Linnean Society*, **68**, 303–316.

Guillaumet A, Pons JM, Godelle B, Crochet PA (2006) History of the Crested Lark in the Mediterranean region as revealed by mtDNA sequences and morphology. *Molecular Phylogenetics and Evolution*, **39**, 645–656.

Guillaumet A, Crochet PA, Pons JM (2008) Climate-driven diversification in two widespread *Galerida* larks. *BMC Evolutionary Biology*, **8**, 32.

Guiller A, Coutellec-Vreto MA, Madec L, Deunff J (2001) Evolutionary history of the land snail *Helix aspersa* in the Western Mediterranean: preliminary results inferred from mitochondrial DNA sequences. *Molecular Ecology*, **10**, 81–87.

Hall TA (1999) BioEdit: a user-friendly biological sequence alignment editor and analysis program for Windows 95/98/NT. *Nucleic Acids Symposium Series*, **41**, 95–98.

Hewitt GM (1999) Post-glacial recolonisation of European biota. *Biological Journal of the Linnean Society*, **68**, 87–112.

Hewitt GM (2004) Genetic consequences of climatic oscillations in the Quaternary. *Philosophical Transactions of the Royal Society of London Series B, Biology Sciences*, **359**, 183–195.

Hijmans RJ, Cameron SE, Parra JL, Jones PG, Jarvis A (2005) Very high resolution interpolated climate surfaces for global land areas. *International Journal of Climatology*, **25**, 1965–1978.

Hijmans RJ, Phillips S, Leathwick J, Elith J (2011) Package 'dismo' for species distribution modeling with R. Available from: http://cran.r-project.org/web/packages/dismo/index.html.

Holm S (1979) A simple sequentially rejective Bonferroni test procedure. *Scandinavian Journal of Statistics*, **6**, 65–70.

Hope AG, Waltari E, Fedorov VB, Goropashnaya AV, Talbot SL, Cook JA (2011) Persistence and diversification of the Holartic shrew *Sorex tundrensis* (Family Soricidae), in response to climate change. *Molecular Ecology*, **20**, 4346–4370.

Idaghdour Y, Broderick D, Korrida A, Chbel F (2004) Mitochondrial control region diversity of the houbara bustard *Chlamydotis undulata* complex and genetic structure along the Atlantic seaboard of North Africa. *Molecular Ecology*, **13**, 43–54.

Illera JC, Richardson DS, Helm B, Atienza JC, Emerson BC (2008) Phylogenetic relationships, biogeography and speciation in avian genus *Saxicola*. *Molecular Phylogenetics and Evolution*, **48**, 1145–1154.

Illera JC, Koivula K, Broggi J, Päckert M, Martens J, Kvist L (2011) A multi-gene approach reveals a complex evolutionary history in the *Cyanistes* species group. *Molecular Ecology*, **20**, 4123–4139.

Illera JC, Rando JC, Richardson DS, Emerson BC (2012) Age, origins and extinctions of the avifauna of Macaronesia: a synthesis of phylogenetic and fossil information. *Quaternary Science Reviews*, **50**, 14–22.

Jolly D, Prentice IC, Bonnefille R *et al.* (1998) Biome reconstruction from pollen and plant macrofossil data for Africa and the Arabian peninsula at 0 and 6000 years. *Journal of Biogeography*, **25**, 1007–1027.

Jost L (2008) GST and its relatives do not measure differentiation. *Molecular Ecology*, **17**, 4015–4026.

Keane TM, Creevey CJ, Pentony MM, Naughton TJ, McInerney JO (2006) Assessment of methods for amino acid matrix selection and their use on empirical data shows that ad hoc assumptions for choice of matrix are not justified. *BMC Evolutionary Biology*, **6**, 29.

Khoury F, Al-Shamlih M (2006) The impact of intensive agriculture on the bird community of a sand dune desert. *Journal of Arid Environments*, **64**, 448–459.

Kröpelin S, Verschuren D, Lézine AM *et al.* (2008) Climate-driven ecosystem succession in the Sahara: the past 6000 years. *Science*, **320**, 765–768.

Kruglyak S, Durrett RT, Schug MD, Aquadro CF (1998) Equilibrium distributions of microsatellite repeat length resulting from a balance between slippage events and point mutations. *Proceedings of the National Academy of Science USA*, **95**, 10774–10778.

Kvist L, Ponnikas S, Belda EJ *et al.* (2011) Decline in population size has different effects to genetic structures in two subspecies of the reed bunting (*Emberiza schoeniclus witherbyi* and *E. s. lusitanica*) in Iberian Peninsula. *Journal of Ornithology*, **152**, 681–693.

Lande R, Engen S, Sæther B-E (2003) *Stochastic Population Dynamics in Ecology and Conservation*. Oxford University Press, Oxford, UK.

Le Houérou HN (2000) Restoration and rehabilitation of arid and semiarid Mediterranean ecosystems in North Africa and West Asia: a review. *Arid Soil Research and Rehabilitation*, **14**, 314.

Librado P, Rozas J (2009) DnaSP v5: a software for comprehensive analysis of DNA polymorphism data. *Bioinformatics*, **25**, 1451–1452.

Llabrés X (2010) Cria possible de pinsà trumpeter *Bucanetes githagineus* a Mallorca. *Anuari Ornitològic de les Balears*, **25**, 51–55.

López-Seoane V (1861) Catálogo de la aves observadas en Andalucía. *Revista de los Progresos de las Ciencias Exactas, Físicas y Naturales*, 1–62.

Luikart G, Cornuet JM (1998) Empirical evaluation of a test for identifying recently bottlenecked populations from allele frequency data. *Conservation Biology*, **12**, 228–237.

MacMillen RE (1990) Water economy of granivorous birds: a predictive model. *The Condor*, **92**, 379–392.

Manrique J, Ballesteros G, Barone R, López-Iborra G (2003) Camachuelo trompetero *Bucanetes githagineus*. *Atlas de las Aves Reproductoras de España* (eds Martí R, del Moral JC), pp. 590–591. DGCONA-SEO/Birdlife, Madrid, Spain.

Martínez JG, Soler JJ, Soler M, Møller AP, Burke T (1999) Comparative population structure and gene flow of a brood parasite, the great spotted cuckoo (*Clamator glandarius*), and its primary host, the magpie (*Pica pica*). *Evolution*, **53**, 269–278.

Myers N, Mittermeier RA, Mittermeier CG, da Fonseca GAB, Kent J (2000) Biodiversity hotspots for conservation priorities. *Nature*, **403**, 853–858.

Nicolas V, Granjon L, Duplantier JM, Cruaud C, Dobigny G (2009) Phylogeography of spiny mice (genus *Acomys*, Rodentia: Muridae) from the south-western margin of the Sahara with taxonomic implications. *Biological Journal of the Linnean Society*, **98**, 29–46.

van Oosterhout C, Hutchinson WF, Wills DPM, Shipley P (2004) MICRO-CHECKER: software for identifying and correcting genotyping errors in microsatellite data. *Molecular Ecology Notes*, **4**, 535–538.

Päckert M, Martens J, Tietze DT, Dietzen C, Wink M, Kvist L (2007) Calibration of a molecular clock in tits (Paridae). Do nucleotide substitution rates of mitochondrial genes deviate from the 2% rule? *Molecular Phylogenetics and Evolution*, **44**, 1–14.

Parmesan C, Yohe G (2003) A globally coherent fingerprint of climate change impacts across natural systems. *Nature*, **421**, 37–42.

Peakall R, Smouse PE (2012) GenAlEx 6.5: genetic analysis in Excel. Population genetic software for teaching and research – an update. *Bioinformatics*, **28**, 2537–2539.

Peterson AT, Soberón J, Sánchez-Cordero V (1999) Conservatism of ecological niches in evolutionary time. *Science*, **285**, 1265–1267.

Phillips SJ, Dudik M (2008) Modelling of species distributions with Maxent: new extensions and a comprehensive evaluation. *Ecography*, **31**, 161–175.

Phillips SJ, Anderson RP, Schapire RE (2006) Maximum entropy modeling of species geographic distributions. *Ecological Modelling*, **190**, 231–259.

Piertney SB, Marquiss M, Summers R (1998) Characterization of tetranucleotide microsatellite markers in the Scottish crossbill (*Loxia scotica*). *Molecular Ecology*, **7**, 1261–1263.

Piry S, Luikart G, Cornuet JM (1999) BOTTLENECK: a computer program for detecting recent reductions in the effective population size using allele frequency data. *Journal of Heredity*, **90**, 502–503.

Pritchard JK, Stephens M, Donnelly P (2000) Inference of population structure using multilocus genotype data. *Genetics*, **155**, 945–959.

Rato C, Brito JC, Larbes S, Shacham B, Harris DJ (2007) Phylogeography and genetic diversity of *Psammophis schokari* (Serpentes) in North Africa based on mitochondrial DNA sequences. *African Zoology*, **42**, 112–117.

Rato C, Carranza S, Perera A, Carretero MA, Harris DJ (2010) Conflicting patterns of nucleotide diversity between mtDNA and nDNA in the Moorish gecko, *Tarentola mauritanica*. *Molecular Phylogenetics and Evolution*, **56**, 962–971.

Raymond M, Rousset F (1995) GENEPOP (version 1.2): population genetics software for exact tests and ecumenicism. *Journal of Heredity*, **86**, 248–249.

Rebelo H, Froufe E, Brito JC *et al.* (2012) Postglacial colonization of Europe by the barbastelle bat: agreement between molecular data and past predictive modelling. *Molecular Ecology*, **13**, 43–54.

Root TL, Price JT, Hall KR, Schneider SH, Rosenzweig C, Pounds JA (2003) Fingerprints of global warming on wild animals and plants. *Nature*, **421**, 57–60.

Rousset F (2008) Genepop'007: a complete reimplementation of the Genepop software for Windows and Linux. *Molecular Ecology Resources*, **8**, 103–106.

Sambrook J, Russell DW (2001) *Molecular Cloning*, 3rd edn. Cold Spring Harbor Laboratory Press, Cold Spring Harbor, New York, USA.

Sanz JJ (2002) Climate change, birds: have their ecological consequences already been detected in the Mediterranean region? *Ardeola*, **49**, 109–120.

Sato A, O'hUigin C, Figueroa F *et al.* (1999) Phylogeny of Darwin's finches as revealed by mtDNA sequences. *Proceedings of the National Academy of Science USA*, **96**, 5101–5106.

Serra G, Abdallah M, Al Qaim G (2006) First breeding record of Trumpeter Finch *Rhodopechys* (*Bucanetes*) *githagineus* in Syria. *Sandgrouse*, **28**, 173–174.

Slatkin M (1995) A measure of population subdivision based on microsatellite allele frequencies. *Genetics*, **139**, 457–462.

Taberlet P, Fumagalli L, Wust-Saucy AG, Cossons JF (1998) Comparative phylogeography and postglacial colonization routes in Europe. *Molecular Ecology*, **7**, 453–464.

Varela S, Rodríguez S, Lobo JM (2009) Is current climatic equilibrium a guarantee for the transferability of distribution model predictions? A case study of the spotted hyena. *Journal of Biogeography*, **36**, 1645–1655.

Vayreda E (1883) *Fauna Ornitológica de la Provincia de Gerona*. Imprenta Paciano Torres, Gerona, Spain.

Viellot LJP (1820) *Faune Française ou Histoire Naturelle, Générale et Particulière des Animaux qui se Trouvent en France*. Le Vrault & Rapet, Paris, Strasburg, Brüssel, France, Belgium.

Waltari E, Hijmans RJ, Peterson AT, Nyári AS, Perkins SL, Guralnick RP (2007) Locating Pleistocene refugia: comparing phylogeographic and ecological niche model predictions. *PLoS ONE*, **2**, e563.

Author information

RB has a general interest in the habitat ecology, biogeography and conservation of vertebrates, including the trumpeter finch, which he studied during his thesis. Recently, he has studied the role of habitat fragmentation in the life history of vertebrates. LK is a docent in molecular ecology and evolution. Her major research interests are the phylogeography and molecular ecology of several Palaearctic bird species. AB is an evolutionary ecologist interested in the study of the effects of climate change on the immune system in extreme environments. FV is interested in host–parasite interactions, sexual selection and expansive processes of birds in relation to human activity and environmental factors. FK is an ornithologist specialized in arid-adapted birds. SV works on species range shifts, community changes across time and Quaternary mammal extinction events. EM is interested in disentangling the role of morphology in explaining species distribution. She is the leader of the project funding this trumpeter finch study.

Data accessibility

Microsatellite data, DNA sequences and their corresponding GenBank Accession nos. are deposited in the CSIC institutional repository (http://digital.csic.es/handle/10261/85523). Geographical coordinates of the locations used to model the ecological niche of the trumpeter finch from its current range are provided in Table S4 (Supporting Information) and the *R*-script for running the ecological niche models are available in GitHub (https://github.com/SaraVarela/Bucanetes).

Supporting information

Additional supporting information may be found in the online version of this article.

Table S1 Samples used, including population of origin, tissue from which the DNA was extracted, source, code (with ring or museum label) and GenBank Accession nos.

Table S2 Primers used to amplify the mitochondrial control region of the trumpeter finch.

Table S3 Geographical coordinates used in the isolation-by-distance analyses.

Table S4 Geographical coordinates of the locations used to model the ecological niche of the trumpeter finch from its current range.

Table S5 AMOVA analyses with different groupings from the microsatellite data.

Table S6 AMOVA analyses with different groupings using mitochondrial DNA.

Fig. S1 Historical scenarios constructed for the coalescence analyses with combined microsatellite and mitochondrial (576 bp fragment) data.